Mechanical Systems and Signal Processing 100 (2018) 360–370

Contents lists available at ScienceDirect

Mechanical Systems and Signal Processing

journal homepage: www.elsevier.com/locate/ymssp

Short communication

The influence of flywheel micro vibration on space camera and vibration suppression

Li Lin [a,b], Tan Luyang [a,b], Kong Lin [a,c], Wang Dong [a,c,*], Yang Hongbo [a]

[a] Changchun Institute of Optics, Fine Mechanics and Physics, Chinese Academy of Sciences, Changchun 130033, China
[b] University of Chinese Academy of Sciences, Beijing 100049, China
[c] Chang Guang Satellite Technology LTD, Changchun 130033, China

ARTICLE INFO

Article history:
Received 21 December 2016
Received in revised form 26 April 2017
Accepted 16 July 2017
Available online 29 July 2017

Keywords:
Flywheel
Micro vibration
Space camera
Vibration isolator
Angular displacement

ABSTRACT

Studied the impact of flywheel micro vibration on a high resolution optical satellite that space-borne integrated. By testing the flywheel micro vibration with six-component test bench, the flywheel disturbance data is acquired. The finite element model of the satellite was established and the unit force/torque were applied at the flywheel mounting position to obtain the micro vibration data of the camera. Integrated analysis of the data of the two parts showed that the influence of flywheel micro vibration on the camera is mainly concentrated around 60–80 Hz and 170–230 Hz, the largest angular displacement of the secondary mirror along the optical axis direction is 0.04″ and the maximum angular displacement vertical to optical axis is 0.032″. After the design and installation of vibration isolator, the maximum angular displacement of the secondary mirror is 0.011″, the decay rate of root mean square value of the angular displacement is more than 50% and the maximum is 96.78%. The whole satellite was suspended to simulate the boundary condition on orbit; the imaging experiment results show that the image motion caused by the flywheel micro vibrationis less than 0.1 pixel after installing the vibration isolator.

0. Introductions

With the rapid development of space technology, the space camera with large aperture and high resolution has played an increasingly important role in the field of civil, commercial, military, and astronomy [1]. However, the micro vibration generated by the spacecraft, such as the flywheel, the control moment gyroscope and the focusing mechanism, would significantly reduce the imaging quality of the space camera [2,3]. The micro vibration of spacecraft is complex with small amplitude, wide spectrum, which is difficult tobe measure and suppress [4,5]. Moreover, large space camera technology involves many disciplines, the existing micro vibration analysis technology and suppression measures are difficult to meet the needs of its development. So the research of the micro vibration analysis method and suppression technology is very important for the development of high resolution optical satellite.

NASA began to study the reasons for the micro vibration in 1980s, and found that the active parts of the satellite will cause micro vibration [6]. A comprehensive summary of the disturbance source of micro vibration generated on spacecraft was made by Eyerman from in 1990, the source of the disturbance is divided into two categories: the internal disturbance of

* Corresponding author at: Changchun Institute of Optics, Fine Mechanics and Physics, Chinese Academy of Sciences, Changchun 130033, China.
E-mail addresses: ucas_lilin@163.com (L. Li), tanluyang66@163.com (L. Tan), CGST2014@163.com (L. Kong), simest@163.com (D. Wang), yanghb@vip.163.com (H. Yang).

http://dx.doi.org/10.1016/j.ymssp.2017.07.029
0888-3270/

the spacecraft and the disturbance caused by the external environment [7]. Laskin and Martin point out that the biggest disturbance source on the spacecraft is the Reaction Wheel Assembly (RAW) and Control Moment Gyroscope (CMG) [8]. According to the vibration test data of the reaction wheel on the Hubble Space Telescope, the empirical model is established in Ref. [9]. Masterson and Miller from MIT, using Matlab developed a set of tools to extract the relevant parameters of the empirical model from the micro vibration test date, which can predict the disturbance spectrum generated by RWA or CMG under different conditions [10]. The micro vibration response of the RWA or CMG, in a remote sensing satellite which was suspended, is measured; the result shows that the effect of the noise on the test results is small under this condition [11].

Generally, satellite platform and space camera were developed by different departments, the whole process involves a number of research units, which makes the study of the whole satellite vibration is more difficult. Aiming at an integrated design of high resolution optical satellite, this paper focuses on the problem of micro vibration of the flywheel. By testing the flywheel micro vibration with six-component test bench, the flywheel disturbance data is acquired. The finite element model of the satellite was established and the unit force/torque were applied at the flywheel mounting position to obtain the micro vibration data of the camera. Then the results of the two parts are integrated to obtain the disturbance characteristics of the micro vibration. Based on this, the flywheel vibration isolator is designed, and the performance of the flywheel is tested. Finally, the whole satellite was suspended to simulate the boundary condition on orbit, the results of imaging test show that the micro vibration of the flywheel has little effect on the image after installing the vibration isolator.

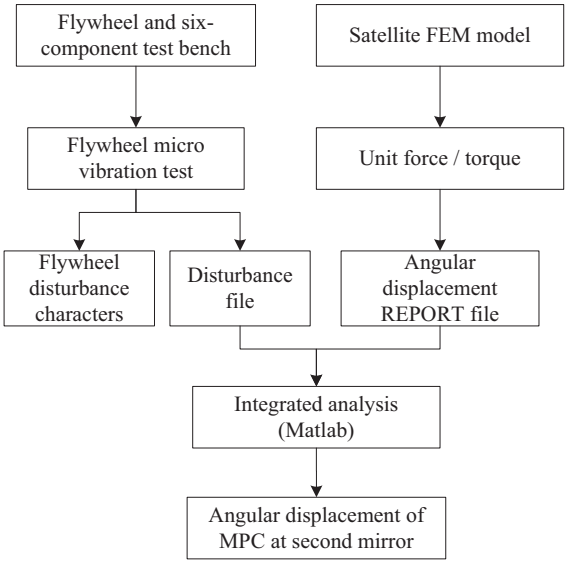

Fig. 1. Flow chart of the influence of micro vibration on the camera.

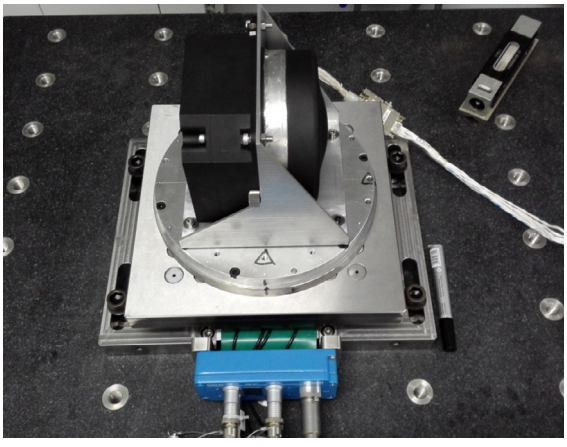

Fig. 2. Test site of flywheel disturbance.

1. Influence of flywheel disturbance on camera

1.1. Analysis process

In this paper, the analysis flow of the impact of micro vibration on a high resolution camera is shown in Fig. 1. Integrated analysis of the measured flywheel disturbance force/torque data and the flywheel unit sine excitation of the angular displacement REPORT files of the satellite, the spectrum characteristics of micro vibration at the secondary mirror (SM) were obtained by MATLAB processing.

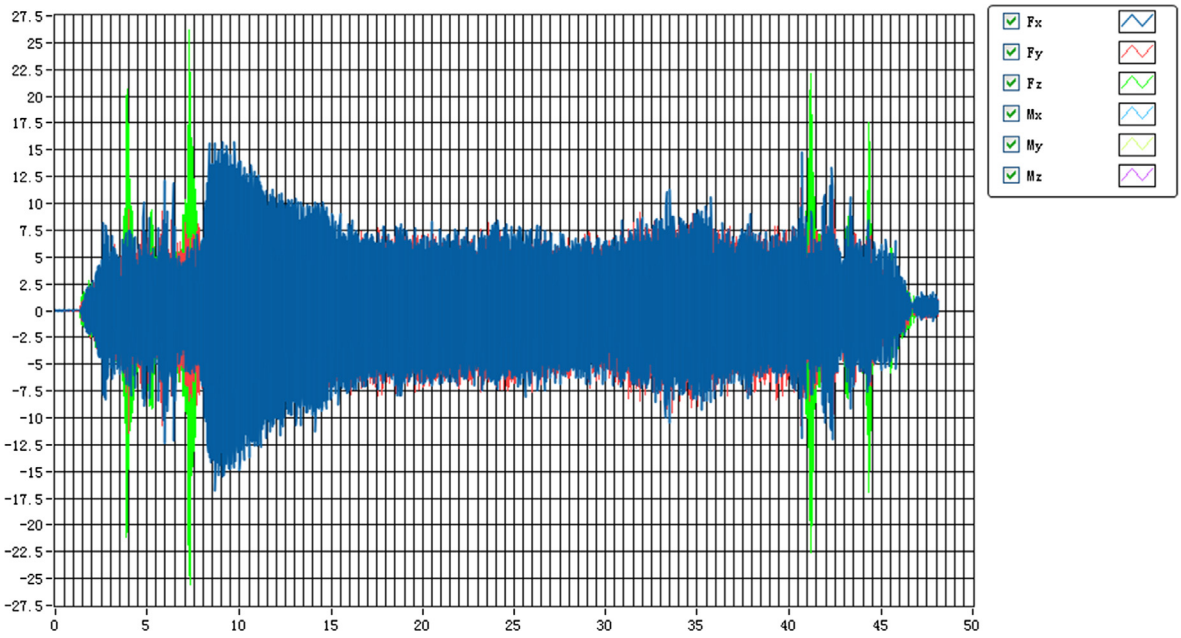

Fig. 3. Typical response curve of flywheel disturbance in time domain.

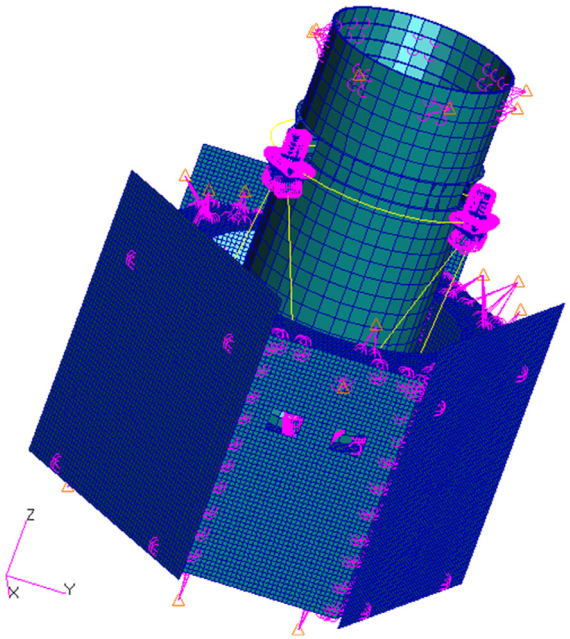

Fig. 4. Satellite FEM.

1.2. Flywheel disturbance test

When the flywheel works normally, it will generate additional disturbance, which will motivate the structure of its first order mode, and the disturbance signal can be greatly enlarged in the frequency domain. It will cause the satellite structure appear micro vibration, and also make the line of sight (LOS) of the camera vibration, which will bring about image distortion and fuzzy [12,13]. The following test was carried out on the flywheel, and the disturbance characteristics were analyzed.

Before the test, the flywheel was installed on the air bearing platform, and then adjusted the level of the floating platform. The disturbance test was carried out in the ultra-clean environment laboratory. The test site is shown in Fig. 2.

The typical response curve of flywheel disturbance in time domain is shown in Fig. 3.

When the satellite is in the position of push broom imaging in orbit, the flywheel spins at a constant speed [14]. Therefore, it is needed to analyze the response characteristics of flywheel disturbance when the test process of the flywheel is stable (such as 20–30 s in Fig. 3).

Intercepted the disturbance force/torque output data when the flywheel spun steady at different speeds, the results extracted as *.dat files after filtering and the FFT transform, which recorded as A.

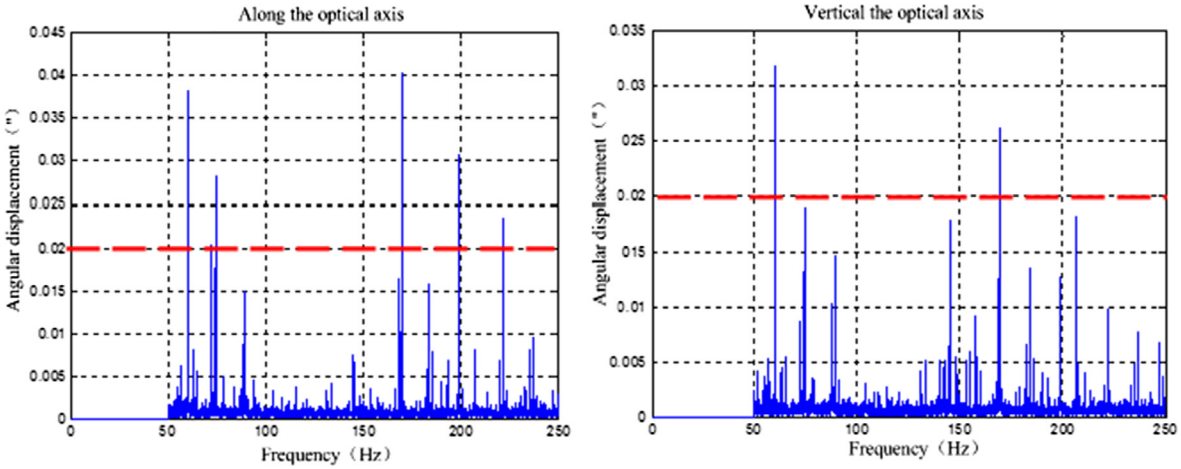

Fig. 5. Micro vibration characteristics of SM.

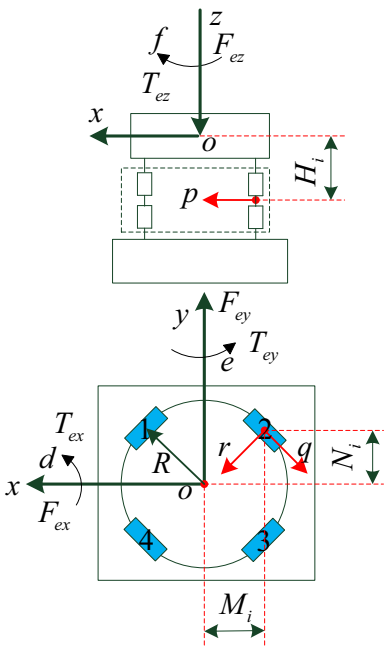

Fig. 6. Schematic diagram of design principle of vibration isolator.

1.3. Micro vibration characteristic analysis of satellite

In order to analyze the micro vibration of flywheel based on the flywheel test date, the finite element model (FEM) of the satellite was established. The definition of the whole satellite coordinates: X axis pointing satellite flight direction, Z axis parallel to the camera optical axis the Y axis is determined by the right hand rule, the FEM shown in Fig. 4.

The flywheel is simulated by lumped mass point, which is connected with the satellite platform by using the finite element model of MPC. The whole satellite FEM model is free from constraints to simulate the Free State in orbit. MPC estab-

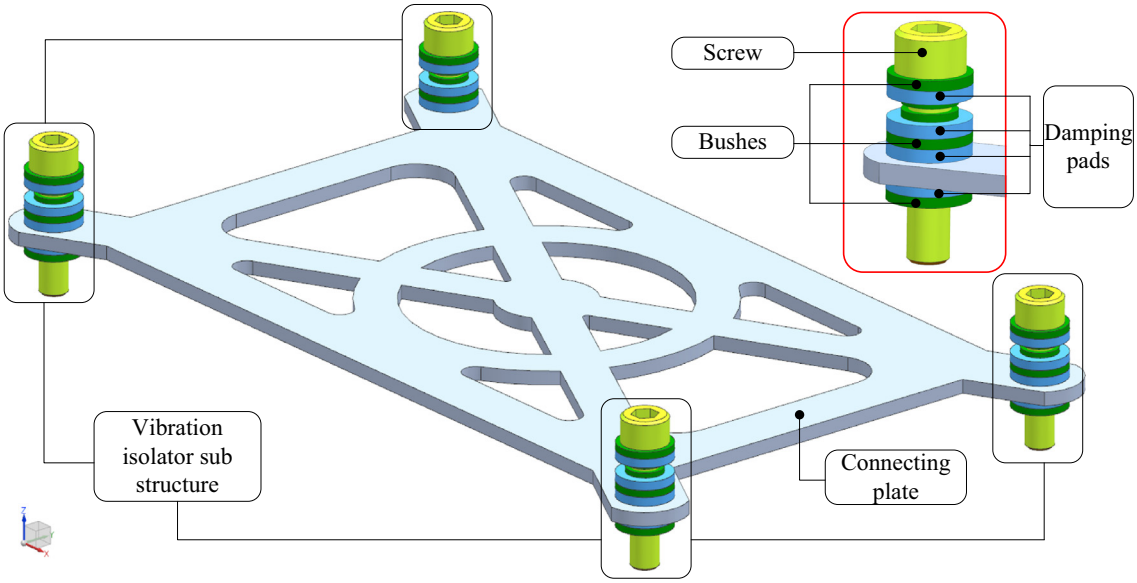

Fig. 7. Artistical model of vibration isolator.

Table 1
Parameters of vibration isolator.

Name	Material	Specification/size (mm)
Screw	TB3	M6 × 35
Bush	TC4	(ϕ6, ϕ8, ϕ16) × (4.5, 2)
Damping pad	Metal-rubber	(ϕ8, ϕ16) × 3
Connecting plate	TC4	190 × 120

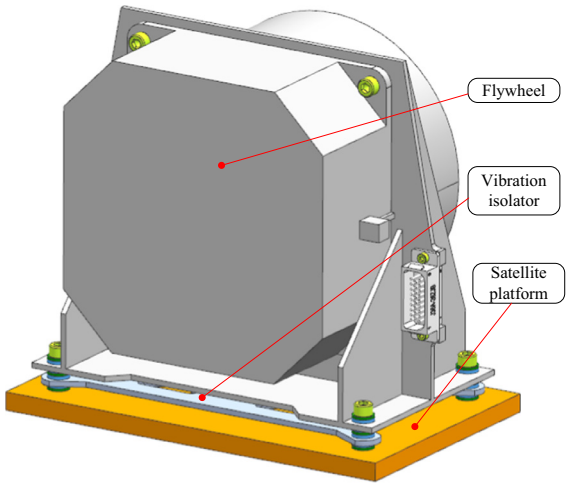

Fig. 8. Relationship between flywheel and vibration isolator and the installation position.

lished in the center of SM, as an analytical study points. Applied unit force/torque at the flywheel centroid and frequency response analysis were carried. Then we obtain the angular displacement of MPC through post-processing. This result was generated as Report file to storage, denoted as B, for the subsequent analysis.

1.4. Flywheel disturbance result

Integrated analysis the flywheel disturbance data A in Section 1.2 and MPC response file B in Section 1.3. After 50 Hz high pass filter [15,16], the micro vibrational spectrum of MPC along the optical axis and the vertical axis is shown in Fig. 5.

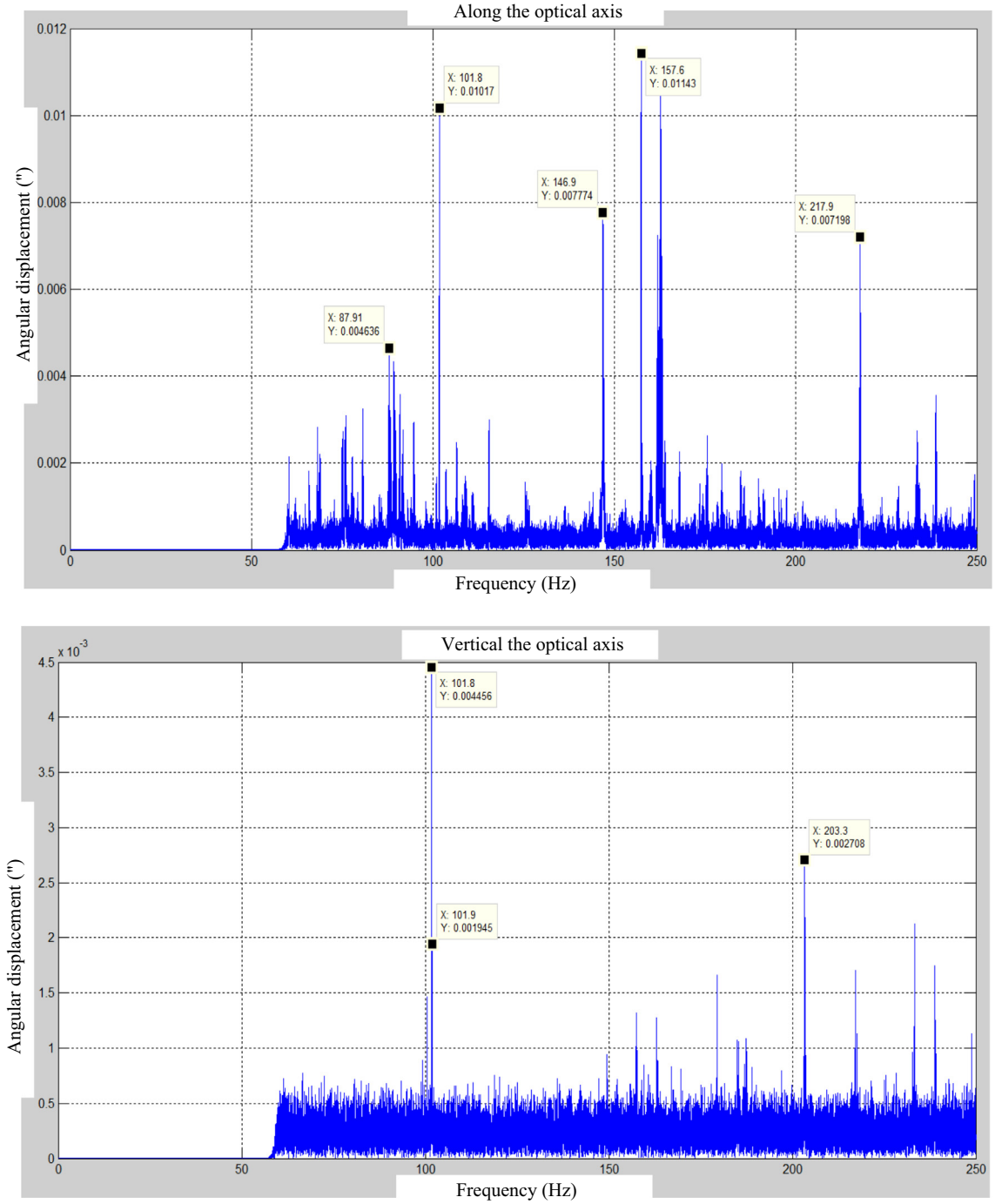

Fig. 9. Micro vibration spectrum of MPC about SM after installing the vibration isolator.

High-resolution camera in this article requires angular displacement response shouldbe less than 0.02″. As shown in Fig. 5, the influence of micro vibration of flywheel on this satellite is mainly focused on 60–80 Hz and 170–230 Hz. The maximum angular displacement along the optical axis reaches 0.04″ in 171 Hz; the maximum angular displacement of the vertical axis reaches 0.032″ in 64 Hz. It can be known that flywheel micro vibration has a great impact on the imaging of the high resolution optical satellite. There are three kinds of flywheel micro vibration solutions: vibration suppression, path optimization and camera isolation design [17–19]. In this paper, the vibration suppression design of the flywheel is carried out.

2. Design of flywheel vibration isolator

2.1. Vibration isolator design principle

The flywheel vibration isolator adopts four point support symmetrical radiation type arrangement, and the vibration isolator is a series of double layer vibration damping design, as shown in Fig. 6. The symmetrical radiation arrangement is characterized in that all the vibration isolator sub structures are uniformly arranged on the same circumference plane, and the two ends are symmetrical. Each substructure has three vertical stiffness; the coupling stiffness of the flywheel damper is zero. The damper can achieve the isolation system of three translations and three rotation direction of the vibration decoupling.

Table 2
Angular displacement RMS 1-sigma data with and without vibration isolator.

Flywheel spinning speed (rpm)	Without vibration isolator		With vibration isolator		Decay rate	
	Along optical axis (″)	Vertical to optical axis (″)	Along optical axis (″)	Vertical to optical axis (″)	Along optical axis	Vertical to optical axis
400	0.027	0.028	0.0104	0.0094	61.48%	66.43%
500	0.043	0.041	0.0147	0.0081	65.81%	80.24%
1000	0.085	0.059	0.0282	0.0019	66.82%	96.78%
1200	0.106	0.067	0.0118	0.0109	88.87%	83.73%
1400	0.065	0.049	0.0087	0.0139	86.62%	71.63%
1500	0.123	0.077	0.0185	0.0182	84.96%	76.36%
1600	0.060	0.052	0.0294	0.0247	51.00%	52.50%
1800	0.112	0.069	0.0186	0.0153	83.39%	77.83%
2000	0.105	0.078	0.0139	0.0158	86.76%	79.74%
2200	0.084	0.052	0.0252	0.0052	70.00%	90.00%
2500	0.086	0.061	0.0180	0.0041	79.07%	93.28%
3000	0.058	0.056	0.0057	0.0040	90.17%	92.86%

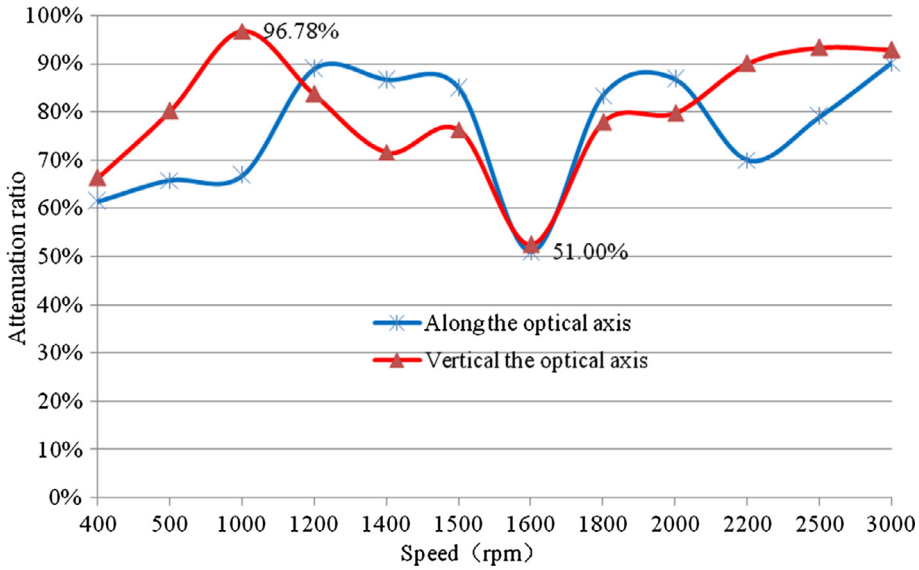

Fig. 10. Decay rate curve of angular displacement of the MPC about SM after installing the vibration isolator.

2.2. Vibration isolator structure

The designed flywheel vibration isolator is shown in Fig. 7. The four vibration isolator sub structures are connected as a complete vibration isolator through the connecting plate, and each sub structure is composed of three bushes, four damping pads and a screw, where in the vibration damping pad is made of metal rubber. After several rounds of optimum design and test, the metal wire diameter of the metal rubber vibration damping pad was determined as 0.15 mm, density was 1.4 g/cm^3, compression rate was 20%, and the damping of the damping pad was 0.04–0.01. Parameters of each component of the vibration isolator are shown in Table 1. The relationship between the flywheel and the vibration isolator and the satellite installation position is shown in Fig. 8.

2.3. Vibration characteristics after installation of vibration isolator

As shown in Fig. 8, installed the vibration isolator, repeated the working process in Chapter 1.2 according to the analysis process in Fig. 1. The disturbance data after the installation of vibration isolator was obtained, which denoted as C. Integrated

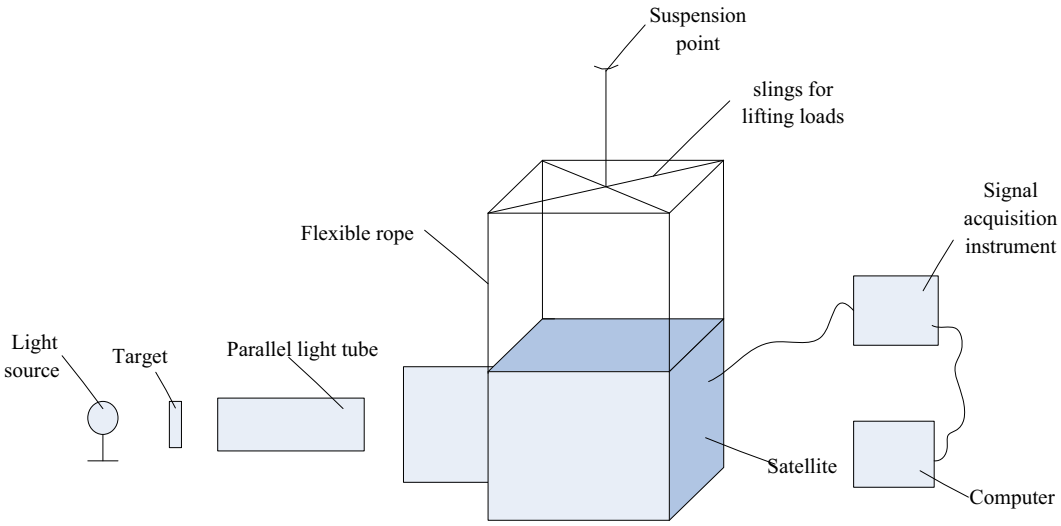

Fig. 11. Schematic diagram of satellite simulation on orbit imaging.

Fig. 12. Effective pixels of the images.

analysis C and B by repeating the analysis process in Chapter 1.4. The micro vibration spectrum of MPC about SM along the optical axis and vertical to the optical axis is shown in Fig. 9.

From Fig. 9, we can see that the maximum angular displacement is 0.011″ at 157.6 Hz along the optical axis, which is much less than 0.02″.

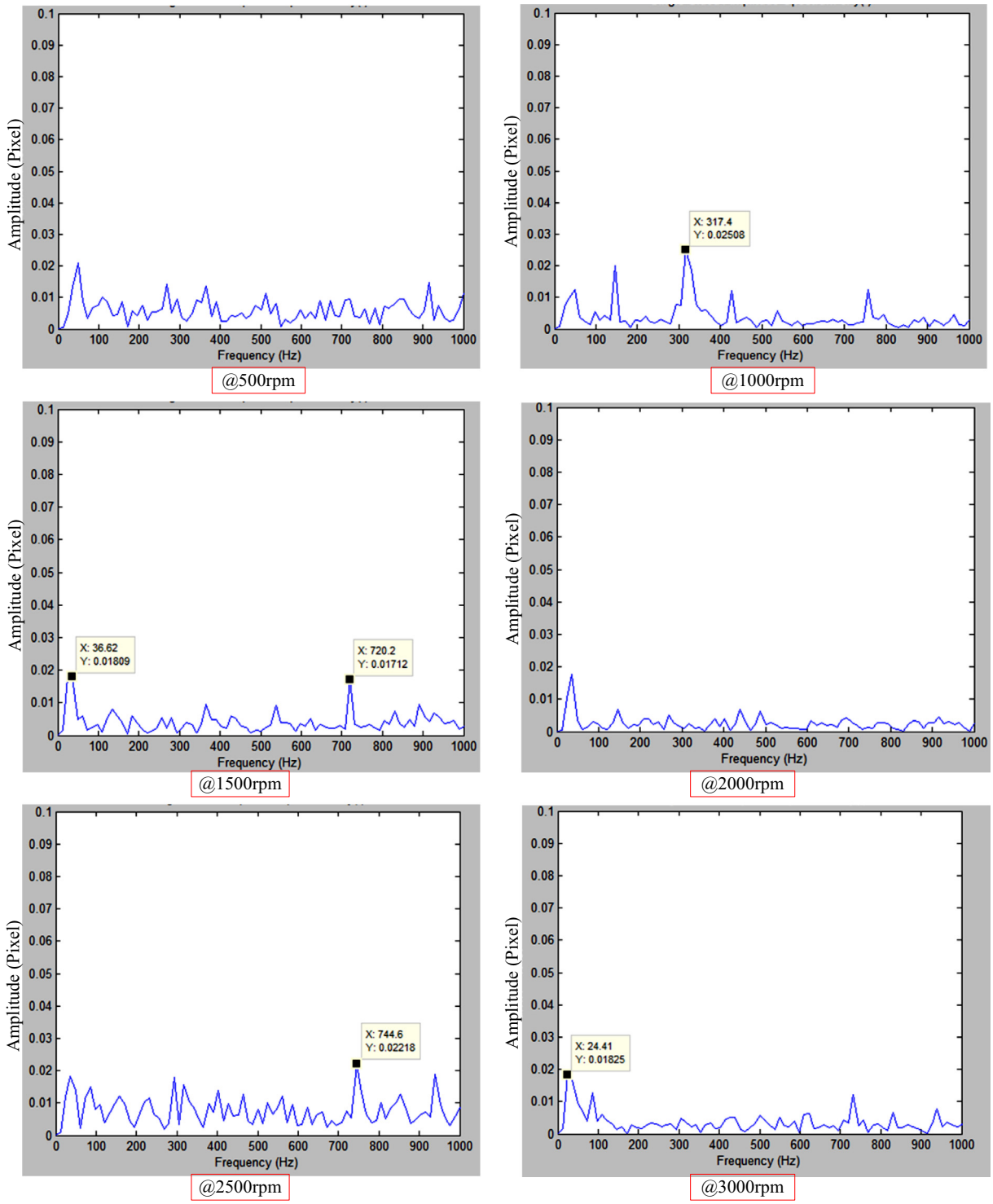

Fig. 13. Amplitude frequency characteristic of the satellite after installing the vibration isolator.

2.4. Comparison of the results before and after the installation of vibration isolator

To further examine the damping effect, the angular displacement root mean square (RMS) 1-sigma data before and after the installation of vibration isolator are listed in Table 2.

The decay rate curve of angular displacement of the MPC about SM after installing the vibration isolator is shown in Fig. 10. The attenuation rate is above 50%, minimum is 51% at 1600 rpm along the optical axis and maximum up to 96.78% at 1000 rpm vertical to axis.

3. Imaging test

In order to verify the effect of flywheel vibration isolator, the satellite is suspended and the camera imaging test is carried out. Test principle is shown in Fig. 11. The satellite suspended at the suspension point through flexible rope sling to simulate the free boundary condition in orbit. The flexible rope natural frequency is less than 1.2 Hz [20,21]. The target is illuminated by the light source through the parallel light tube to simulate the infinite distant object, and then imaging through the satellite. The signal acquisition instrument collects the image of the flywheel at different speeds. The computer is used to process the image collected by the signal acquisition instrument.

The effective pixels (2000 pixel $*$ 55 pixel) of the images of the camera under different rotating speed are analyzed, as shown in Fig. 12. The amplitude frequency characteristic of the satellite after installing the vibration isolator is obtained by Matlab, as shown in Fig. 13.

According to Fig. 13, the amplitude of the camera imaging under different frequencies were less than 0.1 pixel. The image motion caused by micro vibration had no effect on camera imaging [22], which showed that the effect of flywheel vibration isolator is effective.

4. Conclusions

(1) The effect of the flywheel micro vibration on camera imaging mainly concentrated on 60–80 Hz and 170–230 Hz, the maximum angular displacement along the optical axis reached 0.04″ at 171 Hz, and vertical to the optical axis up to 0.032″ at 64 Hz.
(2) Designed the flywheel micro vibration damper, the metal wire diameter of the metal rubber vibration damping pad is 0.15 mm, density is 1.4 g/cm^3, compression rate is 20%, and the damping of the damping pad is 0.04–0.01.
(3) After installing vibration isolator, the secondary mirror reference point angular displacement is 0.011″ at 157.6 Hz along the optical axis, which is far less than the set index 0.02″. The attenuation rate of root mean square value of the angular displacement is above 50%, the minimum is 51% in the 1600 rpm along the optical axis and maximum is up to 96.78% in the 1000 rpm vertical to the axis.
(4) The satellite suspended at the suspension point through flexible rope sling to simulate the free boundary condition in orbit. The amplitude of the camera imaging under different frequencies were less than 0.1 pixel. The image motion caused by micro vibration had no effect on camera imaging, which showed that the effect of flywheel vibration isolator is effective.

Acknowledgements

The authors would like to thank the financial support of The National Natural Science Foundation of China (No. 41501383).

References

[1] H.P. Stahl, M. Postman, G. Mosier, et al. AMTD: Update of Engineering Specifications Derived from Science Requirement for Future UVOIR Space Telescope. SPIE, 91431T-91431T-8, 2014.
[2] T.T. Hyde, K.Q. Ha, J.D. Johnston, et al, Integrated modeling activities for the James Webb Space Telescope: optical jitter analysis, Astronom. Telescope Instrument. (2004) 588–599.
[3] J.M. Hilkert, D.L. Amil, Structural Effects and Techniques in Precision Pointing and Tracking Systems: A Tutorial Overview. SPIE, 7696, 76961C, 2010.
[4] J. Liu, D.Y. Dong, H.W. Xin, et al, Temperature adaptation of large aperture mirror assembly, Opt. Precision Eng. 21 (12) (2013) 3169–3175.
[5] S.A. Uebelhart, Non-Deterministic Design and Analysis of Parameterized Optical Structures During Conceptual Design. Massachusetts Institute of Technology, 2006.
[6] D.K. Kim, Micro-vibration model and parameter estimation method of a reaction wheel assembly, J. Sound Vibr. 338 (2014).
[7] C.E. Eyerman, A Systems Engineering Approach to Disturbance Minimization for Spacecraft Utilizing Controlled Structures Technology: [Master Degree], Massachusetts Institute of Technology, USA, 1990.
[8] R.A. Laskin, M.S. Martin, Control/structure system design of a space borne optical interferometer in: Proceedings of the AAS/AIAA Astrodynamics Specialist Conference, 1989, pp. 369–395.
[9] L.P. Davis, J. Wilson, R. Jewell, et al. Hubble Space Telescope Reaction Wheel Assembly Vibration Isolation System NASA Report N87–22702, 1986, pp. 669–690.
[10] R.A. Masterson, D.W. Miller, R.L. Grogan, Development and validation of reaction wheel disturbance models: empirical model, J. Sound Vibr 249 (3) (2002) 575–598.

[11] Z.Y. Wang, Y.J. Zou, A.C. Jiao, et al, The jitter measurement and analysis for a remote sensing satellite platform, Spacecraft Environ Eng. 3 (32) (2015) 278–285.
[12] Q. Hu, Y.H. Jia, S.J. Xu, Adaptive suppression of linear structural vibration using control moment gyroscopes, J. Guidance, Control, Dyn. 37 (3) (2014) 990–995.
[13] W.Y. Zhou, D.X. Li, Q. Luo, et al, Analysis and testing of micro-vibrations produced by momentum wheel assemblies, Chin. J. Aeronaut. 25 (4) (2012) 640–649.
[14] M. Toyoshima, Y. Takayama, H. Kunimori, In orbit measurements of spacecraft micro-vibrations for satellite laser communication links, Opt. Eng. 49 (8) (2010).
[15] J. Karl, Christopher Pendergast, J. Schauwecker, Use of a passive reaction wheel jitter isolation system to meet the Advanced X-ray Astrophysics Facility imaging performance requirements, SPIE, vol. 3356, 1998, 0277-786X1078-1094.
[16] LailaMireille Elias, Frank Dekens, IpekBasdogan, Lisa Sievers, Tim Neville, A methodology for ‘‘modeling” the mechanical interaction between a reaction wheel and a flexible structure, SPIE, vol. 4852, 2003, pp. 541–555.
[17] Dr. Vanessa Camelo, Dr. Allen Bronowicki, et al., Damping and isolation concepts for vibration suppression and pointing performance, in: 50th AIAA/ASME/ASCE/AHS/ASC Structures, Structural Dynamics, and Materials Conference, Palm Springs, 2009, pp. 1–16.
[18] D. Kamesh, R. Pandiyan, A. Ghosal, Modeling, design and analysis of low frequency platform for attenuating micro-vibration in spacecraft, J. Sound Vibr 329 (17) (2010) 3431–3450.
[19] Zhanji Wei, Dongxu Li, Rui Xu, Vbration isolation research on the metal rubber damping rod of payload attach fitting, J. Adv. Mater. Res. 391–392 (2012) 467–473.
[20] S. Adachi, I. Yamaguchi, et al, On-orbit system identification experiments on engineering test satellite-VI, Control Eng. Pract. 7 (1999) 831–841.
[21] M. Toyoshima, T. Jono, Nobuhiro. Transfer functions of micro vibrational distuibances on a satellite, in: 21st AIAA ICSSC and Exhibit, Yokohama, Japan, 2003.
[22] Pang Shiwei, Pan Teng, Mao Yilan, et al, Study and verification of micro-vibration test for a satellite, Spacecraft Environ. Eng. 33 (3) (2016) 305–311.